HHS Public Access

Author manuscript

J Neurosci Methods. Author manuscript; available in PMC 2017 January 15.

Published in final edited form as:

J Neurosci Methods. 2016 January 15; 257: 204–213. doi:10.1016/j.jneumeth.2015.09.005.

Comparing Prognostic Strength of Acute Corticospinal Tract Injury Measured by a New Diffusion Tensor Imaging Based Template Approach Versus Common Approaches

Kelsi K. Hirai, B.S.[1,2], **Benjamin N. Groisser, B.A.**[1,2], **William A. Copen, M.D.**[2], **Aneesh B. Singhal, M.D.**[3], and **Judith D. Schaechter, Ph.D.**[1,2]

[1]MGH/HST Athinoula A. Martinos Center for Biomedical Imaging, Charlestown, MA

[2]Department of Radiology, Massachusetts General Hospital, Harvard Medical School, Boston, MA

[3]Department of Neurology, Massachusetts General Hospital, Harvard Medical School, Boston, MA

Abstract

Background—Long-term motor outcome of acute stroke patients with severe motor impairment is difficult to predict. While measure of corticospinal tract (CST) injury based on diffusion tensor imaging (DTI) in subacute stroke patients strongly predicts motor outcome, its predictive value in acute stroke patients is unclear. Using a new DTI-based, density-weighted CST template approach, we demonstrated recently that CST injury measured in acute stroke patients with moderately-severe to severe motor impairment of the upper limb strongly predicts motor outcome of the limb at 6 months.

New Method—The current study compared the prognostic strength of CST injury measured in 10 acute stroke patients with moderately-severe to severe motor impairment of the upper limb by the new density-weighted CST template approach versus several variants of commonly used DTI-based approaches.

Results and Comparison with Existing Methods—Use of the density-weighted CST template approach yielded measurements of acute CST injury that correlated most strongly, in absolute magnitude, with 6-month upper limb strength ($r_s = 0.93$), grip ($r_s = 0.94$) and dexterity ($r_s = 0.89$) compared to all other 11 approaches. Formal statistical comparison of correlation coefficients revealed that acute CST injury measured by the density-weighted CST template approach correlated significantly more strongly with 6-month upper limb strength, grip and dexterity than 9, 10 and 6 of the 11 alternative measurements, respectively.

Corresponding Author: Judith D. Schaechter, Ph.D., MGH/HST Athinoula A. Martinos Center for Biomedical Imaging, 13th Street, Building 149, Room 2301, Charlestown, MA 02129, tel: 617.726.5622, fax: 617.726.7422, judith@nmr.mgh.harvard.edu.

Conclusions—Measurements of CST injury in acute stroke patients with substantial motor impairment by the density-weighted CST template approach may have clinical utility for anticipating healthcare needs and improving clinical trial design.

1. Introduction

Accurate prognosis of long-term motor outcome of patients early after stroke would have significant clinical utility in anticipating future healthcare needs and improving the design of clinical trials. While clinical measurement of motor impairment of the upper limb is a relatively good predictor of motor outcome of the limb for acute stroke patients with mild to moderate motor impairment,[1-3] it poorly predicts limb motor outcome for acute stroke patients with severe impairment.[1-5] We recently showed that the extent of corticospinal tract (CST) injury in patients with moderately-severe to severe motor impairment of the upper limb 3-7 days after stroke, measured using a new density-weighted CST template approach that utilizes diffusion tensor imaging (DTI) data, strongly predicts motor outcome of the limb at 6 months.[6] Acute CST injury was measured by the loss in axial diffusivity (AD) of the ipsilesional CST relative to the contralesional CST. We showed that the loss in CST AD was a far stronger prognostic indicator of long-term motor outcome compared to other diffusion abnormalities of the CST, including radial diffusivity (RD) and fractional anisotropy (FA). Furthermore, we showed that the loss in CST AD remained strongly predictive even after adjusting for commonly considered predictors of motor outcome, including age, initial motor impairment or lesion volume. Since AD is the magnitude of dominant diffusivity, and reduced AD has been associated with loss in axonal fiber integrity,[7-9] we interpreted the loss in CST AD at 3-7 days post-stroke as an early indicator of CST axon degeneration. A previous quantitative DTI study in patients 7 days after hemispheric stroke found greater diffusion abnormality in the ipsilesional cerebral peduncle associated with poor motor outcome.[10] However, other studies in patients within one week after hemispheric stroke did not detect a diffusion abnormality in the pontine region of the CST[11] or along the CST from the pons to cerebral peduncle,[12] and thus CST diffusion was not predictive of motor outcome. In contrast, DTI studies that measured CST injury in patients with a stroke incurred weeks to months prior using a variety of approaches have consistently found prognostic value of the loss in CST FA,[8, 13-15] a metric reflecting the relative magnitude of principal diffusivities and most commonly used to measure white matter injury.[16] These findings are explained, in part, by progressive degenerative changes of the CST during the early post-stroke period[17, 18] that ease detection of CST abnormalities by DTI with greater time post-stroke. Moreover, these findings raise the question whether the prognostic value of acute CST injury measurements depends on the DTI-based approach applied. Filling this knowledge gap is most clinically pressing for acute stroke patients with severe motor impairment, those for whom motor outcome is currently difficult to predict.

There are a variety of DTI-based approaches for measuring CST injury and no “gold standard” among them. The three most common can be categorized as CST tractography, CST template, and CST region-of-interest (ROI) approaches. Tractography involves applying an algorithm to a DTI dataset to propagate streamlines based on voxel-based tensor properties.[19] CST streamlines can be localized using anatomical landmarks as endpoints, and quantitative properties measured by diffusion, number or volume.[20-22]

CST template approaches localize a set of common voxels of the CST in a standard brain space, usually MNI space. To accomplish this, CST tractography is applied to DTI datasets from healthy adults, then each set of resultant CST streamlines is aligned to the standard space using an automated registration algorithm and summed voxelwise across subjects. Often, a threshold is applied to the resultant summed volume to create a binary CST template.[23-26] Our density-weighted CST template was constructed similarly, though each voxel was coded by the relative number of CST streamlines rather than a binary number. Once the CST template is constructed, it is used to determine the likely location of the CST in each patient brain by automated registration of the patient's image volume to the template space. Then, properties of each patient's CST can be measured by diffusion[24] or lesion load.[23, 25, 27] The density-weighted CST template approach adds the step of moving the CST template into the patient's DTI space by applying the inverted registration matrix, then refining selection of voxels considered part of the patient's CST prior to measuring CST diffusion.

Lastly, CST ROI approaches involve localizing a specific region of the CST, and this is commonly the posterior limb of the internal capsule (PLIC). ROI (PLIC) localization is often accomplished by manual delineation using expert neuroanatomical knowledge,[28, 29] though some studies utilize CST streamlines[30] or a standardized ROI.[15, 31] Diffusion in the ROI is measured to reflect CST injury.

The current study quantified CST injury in patients with moderately-severe to severe motor impairment of the upper limb at 3-7 days by CST AD based on the new density-weighted CST template approach and several variants of the three common approaches: 1) binary CST template with measurement of CST AD, FA and lesion load; 2) CST ROI with measurement of AD and FA in the PLIC; and 3) CST tractography with measurement of CST AD, FA and fiber number. At six months post-stroke, several aspects of upper limb motor function (i.e., overall strength, grip, dexterity) were measured. Each acute CST injury measurement was correlated against each 6-month motor outcome. Finally, for each motor outcome, the correlation strength against acute CST injury measured by the density-weighted CST template approach was compared to the correlation strength against acute CST injury measured by each alternative approach.

2. Methods

2.1 Subjects

Data for the current study came from 10 acute stroke patients who fulfilled the following criteria: 1) Middle cerebral artery ischemic stroke with onset ≤ one week prior; 2) First symptomatic hemiparetic stroke; 3) Moderately-severe to severe upper limb paresis at the time of acute motor function testing, defined as ≥ 50% loss on all motor function tests (see section 2.2); 4) Participated in follow-up motor function testing 6-months after stroke; 5) Medical stability and cognitive status permitting competent participation in study procedures; and 6) No MRI contraindication. Table 1 provides characteristics of these 10 patients. A voxelwise map of lesion overlap among the patients is provided as Supplementary Material (section 1). In addition, 12 healthy adults were enrolled for imaging in order to create CST templates. These normal subjects were matched roughly to the patient

group for age (50 ± 12 years), gender (9 of 12 male), and handedness (all right hand dominance). All subjects provided written informed consent in accordance with the Human Subjects Committee of the local Institutional Review Board.

2.2 Motor Function Testing

At the acute and 6-month time points, three tests that capture different aspects of motor function of the upper limb were administered: 1) Upper limb section of the Motricity Index (MI-UL; scale 1 – 100), a valid and reliable test of overall limb strength;[32] moderately-severe to severe paresis at the acute time point was defined as scoring ≤ 51. 2) Hand grip strength measured by digital dynamometry[33] in 2 × 5-sec trials with maxima of replicate trials averaged; moderately-severe to severe loss in grip strength at the acute time point was defined as strength of the paretic hand ≤ 50% relative to the contralateral hand. 3) Dexterity measured by the Nine Hole Peg Test[34] (NHPT) in 2 × ≤ 60-sec trials with pegs/sec of replicate trials averaged; moderately-severe to severe loss in dexterity at the acute time point was defined as ≤ 50% pegs/sec of the paretic hand relative to the contralateral hand. In addition, the upper limb motor section of the Fugl-Meyer Stroke Scale (FM-UL, scale 0-66), a valid and reliable assessment of overall motor impairment (i.e., abnormal synergies, strength, coordination and reflexes)[35, 36] was administered to 9 of the 10 stroke patients at the 6-month time point.

2.3. Image Acquisition

Images were acquired using a Siemens 3T TIM Trio MRI scanner and 12-channel head coil. DTI was performed using a twice-refocused echo planar spin-echo sequence (repetition/echo time = 8910/83 ms; flip angle = 90°; field-of-view = 240 × 240 mm; number of slices = 72; slice thickness/gap = 2/0 mm; voxel size = 2 × 2 × 2 mm; number of acquisitions = 70 with 60 non-collinear directions at b-value 700 s/mm^2 and 10 at b-value 0 s/mm^2). A high-resolution T1-weighted volume was also acquired using a multi-echo magnetization prepared rapid gradient echo sequence (repetition time = 2530 ms; echo time$_{1\text{-}4}$ = 1.64/3.4/5.36/7.22 ms; flip angle = 7°; field-of-view = 256 × 256 mm; slice thickness = 1 mm; voxel size = 1 × 1 × 1 mm).

2.4. DTI Data Pre-Processing

For each DTI dataset, eddy current correction was performed using software (eddy_correct) from FMRIB's Diffusion Toolbox.[37] Using the Diffusion Toolkit (DTK),[38] the b-matrix was then rotated relative to the plane of image acquisition prior to voxelwise modeling of the diffusion tensor, generating a volume for each eigenvalue (λ_1, λ_2, and λ_3), FA, apparent diffusion coefficient (ADC), mean B0 and mean diffusion-weighted image (DWI). The dominant diffusivity λ_1 is also known as AD.

2.5. Measuring Acute CST Injury

Acute CST injury was measured using each of the following approaches.

2.5.1. Density-weighted CST template approach—A density-weighted CST template was constructed using the DTI data from the normal subjects, as we described recently in

detail[6] and shown schematically as Supplementary Material (section 2). Described here in brief, using DTK/Trackvis software,[39] we isolated CST streamlines that penetrated precentral gyrus white matter and ipsilateral cerebral peduncle regions of interest. Using tools from the FreeSurfer[40] software package, each precentral gyrus white matter region of interest was automatically labeled 2 mm subcortical to the precentral cortex on the high-resolution T1-weighted volume, then mapped to the subject's DTI data that had been co-registered using the Boundary-Based Registration algorithm.[41] Each peduncle region of interest was manually drawn in native diffusion space at approximately MNI z = -20 mm with reference to the subject's FA and B0 images. Some CST streamlines extended ventral from the peduncle region of interest. Streamlines that penetrated the pontine CST region at approximately MNI z = -40 mm, based on reference to a DTI-based atlas of brainstem white matter[42] and the subject's color-coded orientation map, were considered part of the CST. Each voxel was coded for the number of penetrating streamlines, which we refer to as density. Density-weighted CST streamlines were spatially normalized to MNI space by applying the transformation matrix that registered the subject's B0 volume to the T2-MNI152 brain calculated using nonlinear registration software (FNIRT) from the FSL Library.[43] Spatially-normalized density-weighted CST streamlines from all normal subjects were summed voxelwise, then scaled linearly with the highest density voxel set to 100. To measure acute CST injury in each patient, the density-weighted CST template was mapped from MNI space to the patient's diffusion data in native space using the inverted nonlinear transformation matrix calculated using FNIRT with the abnormal B0 voxels of the stroke lesion masked during optimization. In native diffusion space, for each transverse slice the 10 highest density CST voxels were selected along the ipsilesional and, separately, contralesional tract. Since the CST in the corona radiata and cerebral peduncles is in close proximity to cerebrospinal fluid-filled ventricles, and automated alignment of the CST template to a patient's native diffusion space is imperfect, we removed from each patient's high density CST volume any voxel with ADC $\geq 1.8 \times 10^{-3}$ mm^2/s, which characterizes cerebrospinal fluid. Resultant ipsilesional CST and contralesional CST masks were used to compute mean AD at each transverse slice, which ranged from 55 to 60 slices. Each AD measurement series was interpolated to 60 points, then smoothed by replacing each value with the mean of itself ± 2 adjacent points. The mean of each smoothed 60-point AD series was computed, and finally, the hemispheric difference between the two AD means ($AD_{ipsilesional} - AD_{contralesional}$) was taken to reflect acute CST injury in the patient.

2.5.2. Binary CST template approach—The same CST streamlines used to construct the density-weighted CST template were used to construct binary CST templates. However, all CST voxels from each normal subject were given a value of 1 (with 0 for non-CST voxels) rather than coded by density. Binary CST streamlines were registered to MNI space using two normalization methods. One method applied the nonlinear transformation matrix that registered the subject's B0 volume to the T2-MNI152 brain, as used to construct the density-weighted CST template; we refer to this as the “direct” normalization method. Since DTI data are often registered to MNI space using a high-resolution structural MRI volume as an intermediate, we also used a second normalization method that computed the linear registration between the subject's B0 and T1-weighted volumes using Boundary-based Registration software from the FreeSurfer library[41] and the nonlinear registration between

the subject's T1-weighted volume and T1-MNI152 brain using FNIRT. These linear and non-linear registration matrices were concatenated, then the concatenated matrix applied to the binary CST streamlines to bring them into MNI space; we refer to this as the “yoke” normalization method. Binary CST streamlines were summed voxelwise across all normal subjects in MNI space, with separate templates constructed using direct- and yoke-normalized CST streamlines. For both CST templates, two binaries were generated, one in which CST voxels were retained only where there was overlap by ≥ 6 of 12 subjects, and the other more conservative template with overlap by ≥ 8 of 12 subjects. Patient DTI data were spatially normalized using the two aforementioned methods, with abnormal intensity voxels of the lesion masked during nonlinear optimization. In MNI space, each of the four binary CST templates was used to compute mean AD of the ipsilesional CST and contralesional CST, and the difference in CST AD calculated for measurement of acute CST injury (i.e., same metric as for density-weighted CST template). Since quantitative DTI studies often measure CST injury using the FA metric, we also calculated the difference in CST FA using the binary CST templates. Furthermore, since CST injury is often measured using hemispheric asymmetry in CST diffusion, we also calculated CST asymmetry by $(diff_{contralesional} - diff_{psilesional})/(diff_{contralesional} + diff_{ipsilesional})$, where diff = mean AD or mean FA.

2.5.3. CST lesion load approach—The CST lesion load approach measured the overlap in MNI space between the patient's infarct and the four aforementioned binary CST templates, direct-and yoke-normalized with 6/12 and 8/12 subject overlap. Each patient's lesion was labeled in MNI space primarily using the DWI volume, with the B0 volume used to clarify lesion borders when needed, separately for direct-normalized and yoke-normalized DTI data. The volume of overlap between the label and binary CST template was determined. Lesion load was computed in percent, with overlap volume divided by total volume of the right or left binary CST, matched for side of infarct. Because of some uncertainty in lesion borders, an investigator labeled the lesion twice with an interval of at least three days and blinded to the first label. If the two lesion load measurements differed by >10% (occurred in 3 of 10 patients using direct-normalized DTI data, and 4 of 10 patients using yoke-normalized DTI data), then the investigator labeled the lesion for a third time while blinded to the two other labels. Final CST lesion load was taken as the mean of two or three measurements for each binary CST template.

2.5.4. CST region-of-interest approach—Axial slices of each patient's color-coded (RGB) DTI volume were visualized using Trackvis software. Voxels of the PLIC that were blue in color, indicating diffusion primarily in the superior-inferior direction, were labeled manually. Each label spanned three slices from the level of the anterior commissure and the two immediately superior slices. If the ipsilesional PLIC did not appear blue because of ischemic injury, the label was drawn to mirror the contralesional PLIC. The labels were used to compute mean AD and mean FA of the ipsilesional and contralesional PLIC. Because of some uncertainty in PLIC borders, an investigator labeled each PLIC pair twice with an interval of at least three days and blinded to the first pair. If the two mean AD or FA measurements differed by > 0.1 (occurred in 1 of 10 patients), then a third pair of labels was drawn, blinded to the other pairs. Final PLIC diffusion was taken as mean diffusion of the

two or three measurements. Difference and asymmetry in PLIC AD and FA were computed using equations provided in sections 2.5.1 and 2.5.2, respectively.

2.5.5. CST tractography—Using DTK/Trackvis software, interpolated streamline tracking was initiated in all brain voxels of each patient's DTI data in native space. Tracking was terminated where FA > 0.15 or angle threshold > 20°. A standardized protocol using a two ROI approach was used to isolate CST streamlines from all resultant streamlines.[44] The cerebral peduncles were labeled on the patient's B0 volume at the most inferior axial slice where the interpeduncular fossa was evident. These labels were used to isolate streamlines that penetrated the ipsilesional and contralesional cerebral peduncles from all streamlines in the brain. Each set of streamlines was inspected to locate a bifurcation in the central sulcus region, with an anterior bundle penetrating the precentral gyrus. Then, a ROI was drawn at the axial slice just superior to the bifurcation, resulting in selection of CST streamlines penetrating the peduncle and ipsilateral precentral gyrus. The number of streamlines between the two ROIs was recorded, and fiber number asymmetry computed by the equation given in section 2.5.2. Voxels of each set of CST streamlines were also converted to a label and used to compute mean AD and FA. Difference and asymmetry in CST AD and FA were computed using equations in sections 2.5.1 and 2.5.2, respectively. When no ipsilesional CST streamline was detected due to ischemic injury (occurred in 2 of 10 patients), fiber number, mean AD and mean FA were recorded as 0.

2.6. Statistical Analyses

The Wilcoxon Signed Rank test was used to evaluate change in motor functions scores between the acute and 6-month time points. With an eye toward comparing prognostic strength of acute CST injury measured by the density-weighted CST template approach to several alternative approaches, we conducted the following correlation analyses in turn, each using Spearman's correlation. First, for each alternative approach, we evaluated “within-approach” correlations in CST injury measurements when selected parameters were varied (i.e., hemispheric imbalance metric; binary CST template threshold; spatial normalization method; diffusion metric). Second, “between-approach” correlations were evaluated to compare CST injury measurements derived using the density-weighted CST template approach versus each alternative approach. Third, we evaluated correlations between acute CST injury measured by each approach and each 6-month motor outcome. Finally, for each motor outcome, we compared the correlation strength of CST injury measurements made by the density-weighted CST template approach to the correlation strength of CST injury measurements made by each alternative approach using the following equation developed by Meng and colleagues to test the difference in correlated correlation coefficients.[45]

$$Z=(z_{r1}-z_{r2})\sqrt{\frac{N-3}{2(1-r_x)h}} \quad (1)$$

where N is the number of subjects, z_{ri} is the Fisher z-transformed $r_i \equiv r_{YXi}$, r_x is the correlation between two predictor variables X_1 and X_2 (i.e., $r_{x_1x_2}$),

$$h=\frac{1-f\overline{r^2}}{1-\overline{r^2}}, \text{and} \quad (2)$$

$$f=\frac{1-r_x}{2(1-\overline{r^2})} \quad (3)$$

Alpha was set at the two-tailed 0.05 level for all statistical testing, with p-values associated with correlation coefficients (r_s) and Meng's z-values corrected for multiple comparisons using the False Discovery Rate (FDR) method.[46]

All testing was conducted using JMP software (SAS Institute Inc., v8.0.2), with two exceptions. The formula function in Microsoft Excel (v12.3.6) was computed to compute Meng's z-values. Software from the Neuroimaging Informatics Tools and Resources Clearinghouse (NITRC) was used to compute FDR-corrected p-values.[47]

3. Results

3.1. Acute and 6-Month Motor Functions

Figure 1 shows scores for MI-UL, grip strength and NHPT at the acute and 6-month post-stroke time points. Patients made significant gains in MI-UL and grip strength over time ($P < 0.01$, Wilcoxon Signed Rank), but not NHPT ($P = 0.125$). No motor function measured at the acute time point correlated significantly with the respective motor function at 6 months (MI-UL $r_s = 0.46$; grip $r_s = 0.37$; NHPT r_s = undefined since there was no variability at the acute time point). Six-month FM-UL scores are provided as Supplementary Material (section 3).

3.2. Within-Approach Correlations of Acute CST Injury Measurements

For each alternative approach, we evaluated correlations between CST injury measurements with one or more parameters varied (Table 2). For the binary CST template, CST ROI and CST tractography approaches, CST injury computed using ‘difference’ as the hemispheric imbalance metric correlated strongly with CST injury computed using the ‘asymmetry’ metric (median $r_s = 0.99$; range $r_s = 0.81$-1.00; 12 comparisons with constant diffusion metric and normalization method). Similarly, for the binary CST template and CST lesion load approaches, CST injury measured using the 6/12 subject overlap template correlated strongly with CST injury measured using the 8/12 subject overlap template (median $r_s = 0.95$; range $r_s = 0.85$-0.99; 10 comparisons with constant diffusion metric and normalization method). In contrast, for the binary CST approach and CST lesion load approaches, CST injury measurements that utilized the direct normalization method correlated only moderately with injury measurements that utilized the yoke normalization method (median $r_s = 0.76$; range $r_s = 0.62$-0.92; 10 comparisons with constant hemispheric imbalance metric, subject overlap and diffusion metric). Furthermore, for the binary CST template, CST ROI and CST tractography approaches, CST injury measured using the AD metric correlated weakly with CST injury measured using the FA metric (median $r_s = 0.22$; range $r_s = 0.05$-0.47; 12 comparisons with constant binary threshold, normalization method and

hemispheric imbalance metric). These findings indicate that CST injury measurements that utilized the 'difference' metric of hemispheric imbalance were redundant with those that utilized the 'asymmetry' metric, and measurements derived using the binary CST template with 6/12 subject overlap were redundant with those derived using the 8/12 subject overlap template. However, CST injury measurements that utilized the two normalization methods (direct and yoke) and two diffusion metrics (AD and FA) were at least moderately dissimilar from one another.

3.3. Between-Approach Correlations of Acute CST Injury Measurements

In face of the redundancies in alternative measurements of acute CST injury described in section 3.2, along with an effort to reduce the number of between-approach comparisons, we elected to eliminate from consideration alternative measurements that used the asymmetry metric (except asymmetry in CST tractography fiber number) and binary CST template with 8/12 subject overlap. Table 3 shows that of the remaining 11 alternative measurements of acute CST injury, AD differences measured by the density-weighted CST template approach correlated most strongly with AD differences measured by the binary CST template using direct and yoke normalization methods (r_s = 0.80 and 0.76, respectively). However, these alternative measurements of acute CST injury did not correlate significantly with measurements made using the density-weighted CST template approach after correction for multiple comparisons using the FDR method.

3.4. Acute CST Injury Related to 6-Month Motor Functions

Figure 2 shows correlations between acute CST injury measured by each approach (with parameter variation as described) and each 6-month motor function of the upper limb. The density-weighted CST template approach yielded measurements of AD difference that correlated significantly with each 6-month motor function (MI-UE r_s = 0.93, grip r_s = 0.94; NHPT r_s = 0.89; corrected $P < 0.01$ for each). AD differences measured by the density-weighted CST template approach also correlated significantly with 6-month FM-UL scores (r_s = 0.94, corrected $P < 0.01$; Supplementary Material, section 4). These correlation strengths indicate that AD difference measured using the density-weighted CST template approach accounted for approximately 79-88% of the variance in motor outcome (i.e., R^2). Scatterplots of the relationship between AD difference measured by the density-weighted CST template approach and each 6-month motor function are provided as Supplementary Material (section 5).

Figure 2 also shows that, unlike AD differences measured by the density-weighted CST template approach, no alternative measurement of acute CST injury correlated significantly with all three 6-month motor functions. AD differences measured by the binary CST template approach correlated significantly with grip strength and NHPT scores but not MI-UL scores when the direct normalization method was applied, and correlated significantly with MI-UL scores and grip strength but not NHPT scores when the yoke normalization method was applied. CST lesion load measurements, when direct or yoke normalization was applied, correlated significantly only with 6-month NHPT scores. Tractography-based measurements did not correlate significantly with any 6-month motor function regardless of whether data from all 10 patients were used in the computations or only data from the 8

patients with successful tracking of ipsilesional CST streamlines (see section 2.5.5 and Supplementary Material section 6).

Figure 2 also shows results of Meng's test used to compare correlation strengths between 6-month motor outcomes (MI-UL, grip, NHPT) and acute CST injury measurements based on the density-weighted CST template approach versus each alternative approach. Across the 6-month motor functions, the correlation with AD differences measured by density-weighted CST template was not significantly stronger than with AD differences measured by the binary CST approach, with one exception (correlation with grip strength when the binary CST approach applied the yoke normalization method). For 6-month MI-UE and grip, but not NHPT, AD differences measured by the density-weighted CST template approach correlated significantly more strongly than CST lesion load regardless of normalization method. For all 6-month motor functions, the correlation with AD differences measured by the density-weighted CST template approach was significantly stronger than the correlation with AD differences measured by the CST ROI and tractography approaches, with one exception (correlation between NHPT and AD differences measured by the ROI approach). For all 6-month motor functions, the correlation with AD differences based on the density-weighted CST template approach was significantly stronger than the correlation with FA differences based on the binary CST template, ROI and tractography approaches. Similar to these aforementioned findings related to MI-UL, grip and NHPT outcomes, AD differences measured by the density-weighted CST template approach correlated significantly more strongly with 6-month FM-UL scores than all other alternative measurements, with one exception (correlation with AD differences measured by the binary/yoke CST approach; Supplementary Material, section 3).

4. Discussion

The current study compared the correlation strength of CST injury measured in acute stroke patients with moderately-severe to severe motor impairment by a new density-weighted CST template approach versus several other commonly used DTI-based approaches. We found that measurements of acute CST injury made by the density-weighted CST template approach correlated most strongly with each 6-month motor function tested (MI-UL, grip, NHPT), with correlation coefficients ranging from 0.89 to 0.94 (each corrected $P < 0.01$), corresponding to explaining 79% to 88% of the variance in outcome scores. Formal statistical comparison of correlation coefficients using Meng's test (Equation 1) revealed that AD difference measurements made by the density-weighted CST template approach correlated with 6-month MI-UE scores significantly more strongly than nine of 11 alternative measurements; correlated with 6-month grip strength significantly more strongly than 10 of 11 alternative measurements; and correlated with 6-month NHPT scores significantly more strongly than six of 11 alternative measurements. These findings suggest that the density-weighted CST template approach yields measurements of CST injury in acute stroke patients with substantial motor impairment that associate strongly with long-term motor outcomes of the upper limb, and that these associations are significantly stronger than with measurements of acute CST injury made by most commonly used DTI-based approaches.

Among the 12 measurements of acute CST injury, only AD differences measured by the density-weighted CST template approach correlated significantly with all three 6-month motor functions. The similar correlation strengths of AD difference measurements made by the binary and density-weighted CST template approaches may have stemmed from both using a template constructed from normalized CST streamlines from healthy adults. The stronger correlations of AD differences based on the density-weighted CST template approach compared to the binary CST template approach (albeit reaching significance in only one of six comparisons) may have resulted from strategies utilized in the new approach that reduced error in the CST AD measurements. These strategies include measuring CST AD in patients' native diffusion space, after inverse warp of the density-weighted CST template from MNI space, allowing for patient-specific selection of most probable (i.e., highest density) CST voxels while avoiding cerebrospinal fluid-filled voxels that often abut the CST in the corona radiata and cerebral peduncle. In contrast, measurements of CST AD made using the binary CST template approach in MNI space may be more contaminated by partial volume effects due to voxels containing both cerebrospinal fluid and CST, an effect that may be exacerbated by the spatial smoothing of DTI data that occurs during the normalization process. The lack of significant difference between the other five of six correlations relates to the moderately strong correlation between AD difference measurements derived from the density-weighted versus binary CST template approaches (r_s = 0.76-80), as Meng's z-statistic is inversely related to the correlation between the two predictors (see Equation 1).

Acute CST lesion load measurements correlated only modestly with 6-month MI-UL scores and grip strength (range r_s =0.38-0.57, NS), while correlated more strongly with 6-month NHPT scores (direct normalization, r_s = 0.84, corrected P = 0.01; yoke normalization, = 0.75, corrected P < 0.05). CST lesion load in each patient was measured by overlap between the volume of DWI abnormality and binary CST template. Previous studies have shown that DWI lesion volume typically increases during the first week after stroke onset.[48, 49] This change in DWI lesion volume may have rendered CST lesion load measured at a single time point 3-7 days post-stroke an unreliable indicator of acute CST injury and thus a relatively weak correlate of 6-month MI-UL scores and grip strength. However, gross differences in DWI lesion volume, and hence CST lesion load measurements, at 3-7 days across our study patients appears to have been a sufficiently good predictor of 6-month NHPT scores that reflect no or minimal dexterity (see Figure 1 and Supplementary Material section 4).

CST AD differences measured by the density-weighted CST template approach correlated with each motor outcome significantly more strongly than CST FA differences measured by all alternative approaches. These findings are consistent with the weak prognostic strength of acute loss in CST FA we reported previously when measured by the density-weighted CST template approach[6] and others have reported when measured by a ROI approach[11] or CST tractography approach.[12] They are also consistent the poor correlation between AD differences measured by the density-weighted CST template approach and FA differences measured by alternative approaches evaluated in the current study (range r_s = 0.16-0.39). While previous DTI studies have demonstrated the prognostic strength of loss in CST FA in patients weeks to months after stroke,[8, 13-15] the current study reiterates our previous finding

of greater prognostic strength of loss in CST AD than CST FA in severely impaired patients within the first week after stroke.

The CST AD differences measured by the density-weighted CST template approach correlated more strongly with each motor outcome than the ROI (PLIC) approach, reaching statistical significance for MI-UL scores and grip strength, but not NHPT scores. This difference in prognostic strength may relate to the varying location of primary CST damage among study patients. Diffusion abnormalities are more profound at the site of primary CST damage than along spared CST.[18, 50] Accordingly, the magnitude of loss in PLIC AD is likely highly dependent on the presence and extent of primary damage to the region, which may render AD measured by the ROI approach a less reliable prognostic indicator than AD measured over the whole CST by the template approach.

Lastly, we found that AD loss and fiber asymmetry measured by CST tractography correlated weakly with each motor outcome (r_s = 0.12-0.43), and AD loss measured by the density-weighted CST template approach correlated significantly stronger with each outcome. The weak correlation strength of these CST tractography measures may be due to the relatively large CST lesions in our study patients, which increases the likelihood that CST tractography fails at voxels with significant diffusion abnormality.[51] Fiber asymmetry based on CST tractography has been used to measure severity of CST injury in chronic patients with relatively small primary lesions to the CST.[22, 52] However, fiber asymmetry may not well differentiate CST injury among patients with large CST lesions when tractography results in few, if any, ipsilesional CST streamlines. Equally problematic, indexing CST injury by diffusion of CST streamlines in patients with large CST lesions may underestimate the injury because diffusion of successfully tracked, not failed, CST streamlines, is measured. A recent DTI study in subacute stroke patients found that CST FA measured by a tractography approach was higher than CST FA measured by a template approach,[53] which may reflect an underestimation in the CST abnormality measured by tractography.

The current study has several strengths and limitations. Its strengths include comparing the correlation strength of acute CST injury measurements made by the recently developed density-weighted CST template approach to a large, albeit not exhaustive, set of alternative DTI-based approaches commonly used for measuring CST injury. A limitation of this study is that we developed the density-weighted CST template approach and compared its prognostic value using the same patient dataset. However, we used several strategies in order to fairly compare prognostic strengths. First, for the current study, we re-measured CST AD difference in each patient using the density-weighted CST template approach. Second, since selection of user-defined parameters of the alternative approaches could affect prognostic strength of resultant measurements, we tested effects of varying several of these parameters (i.e., spatial normalization method, subject overlap threshold, hemispheric imbalance metric, diffusion metric). Third, given potential inaccuracies in delineating the lesion for the CST lesion load approach and ROI (PLIC) approach, we worked to minimize measurement error by taking the mean of duplicate measurements or triplicate measurements (when the difference between the first two measurements was > 10%). The

current study is limited by the small sample size. A validation study involving a larger group of acute stroke patients with severe motor impairment is needed.

In the future, the density-weighted CST template approach could be extended in several ways. One extension could be to fully automate application of the CST template to measure CST injury in acute stroke patients. Currently, the only step requiring manual intervention is labeling of abnormally hyperintense voxels of the lesion in the DTI B0 volume, done to mask these voxels during spatial registration to the T2-MNI152 brain. With recent advances in automated delineation of ischemic tissue,[54, 55] manual labeling could be obviated in the future, saving substantial time and effort.

A second future direction could be to explore the prognostic value of measurements of injury to limb-specific regions of the CST and sensorimotor tracts terminating in regions other than the precentral gyrus. The current density-weighted template was constructed using CST streamlines that penetrated anywhere along the mediolateral swath of white matter beneath the precentral gyrus, which includes motor representations of the lower limb (medial aspect) and upper limb (lateral aspect). However, we found that the majority of reconstructed CST streamlines penetrated the medial aspect of precentral gyrus white matter, with relatively few penetrating the lateral aspect. This pattern is entirely consistent with prior studies using DTI-based CST tractography, and is due to the single tensor model inadequately reflecting multiple fiber orientations in voxels containing crossing fibers, leading to more frequent interruption of CST streamlines extending to the lateral versus medial aspect of the precentral gyrus.[56, 57] Recent advances in tensor-free modeling of fiber orientation, such as constrained spherical deconvolution, have shown improved ability of CST streamlines to penetrate the lateral precentral gyrus compared to DTI-based tractography.[57, 58] Accordingly, a future study might apply tensor-free modeling then tractography to construct density-weighted CST templates specific for the upper and lower limbs (i.e., using lateral and medial precentral gyrus white matter regions of interest, respectively). The prognostic strength of injury measurements made using the newly constructed limb-specific CST templates and the original CST template would then be compared. Tensor-free modeling could also be used to construct density-weighted templates for non-precentral gyrus tracts involved in motor function, including those terminating in the supplementary motor area and postcentral gyrus. The added prognostic value of measurements made using these density-weighted non-precentral gyrus templates could be evaluated.

5. Conclusions

The current study suggests that measurements of CST injury in acute stroke patients with substantial motor impairment made by a new density-weighted CST template approach more strongly associate with long-term motor outcomes of the upper limb than measurements made by all other DTI-based approaches considered here, significantly so in most cases. As acute CST injury measured by the density-weighted CST template approach was found to explain the majority (approximately 85%) of the variance in upper limb motor outcomes, such measurements could provide substantial clinical utility. Clinicians could more confidently inform patients with moderately-severely to severe motor impairment and their

families about expected outcomes. The healthcare system could better project long-term healthcare needs and allocate resources. Clinical trialists could design more efficient acute stroke trials by using this prognostic indicator in patient selection or randomization, and as a surrogate biomarker for long-term motor outcome.

Supplementary Material

Refer to Web version on PubMed Central for supplementary material.

Acknowledgments

This study was supported by grants from the Founders Affiliate of the American Heart Association (09GRNT2240036 to JDS); MGH Executive Committee on Research (to JDS); and NIH-NINDS R01NS051412, P50NS051343, R21NS077442, R21-NS085574 and U10-NS086729 (to ABS). This research was carried out using resources provided by the Biomedical Technology Program of the NIH-NCRR (P41RR14075) and a Shared Instrumentation Grant (1S10RR023043). Statistical consultation was provided with support from Harvard Catalyst | The Harvard Clinical and Translational Science Center (National Center for Research Resources and the National Center for Advancing Translational Sciences, National Institutes of Health Award UL1 TR001102) and financial contributions from Harvard University and its affiliated academic healthcare centers. The content is solely the responsibility of the authors and does not necessarily represent the official views of Harvard Catalyst, Harvard University and its affiliated academic healthcare centers, or the National Institutes of Health.

References

1. Prabhakaran S, Zarahn E, Riley C, Speizer A, Chong JY, Lazar RM, Marshall RS, Krakauer JW. Inter-individual variability in the capacity for motor recovery after ischemic stroke. Neurorehabil Neural Repair. 2008; 22:64–71. [PubMed: 17687024]
2. Zarahn E, Alon L, Ryan SL, Lazar RM, Vry MS, Weiller C, Marshall RS, Krakauer JW. Prediction of motor recovery using initial impairment and fMRI 48 h poststroke. Cereb Cortex. 2011; 21:2712–21. [PubMed: 21527788]
3. Winters C, van Wegen EE, Daffertshofer A, Kwakkel G. Generalizability of the proportional recovery model for the upper extremity after an ischemic stroke. Neurorehabil Neural Repair. 2015; 29:614–22. [PubMed: 25505223]
4. Wade DT, Langton-Hewer R, Wood VA, Skilbeck CE, Ismail HM. The hemiplegic arm after stroke: measurement and recovery. J Neurol Neurosurg Psychiatry. 1983; 46:521–4. [PubMed: 6875585]
5. Binkofski F, Seitz RJ, Hacklander T, Pawelec D, Mau J, Freund HJ. Recovery of motor functions following hemiparetic stroke: a clinical and magnetic resonance-morphometric study. Cerebrovasc Dis. 2001; 11:273–81. [PubMed: 11306779]
6. Groisser BN, Copen WA, Singhal AB, Hirai KK, Schaechter JD. Corticospinal tract diffusion abnormalities early after stroke predict motor outcome. Neurorehabil Neural Repair. 2014; 28:751–60. [PubMed: 24519021]
7. Song SK, Sun SW, Ju WK, Lin SJ, Cross AH, Neufeld AH. Diffusion tensor imaging detects and differentiates axon and myelin degeneration in mouse optic nerve after retinal ischemia. Neuroimage. 2003; 20:1714–22. [PubMed: 14642481]
8. Thomalla G, Glauche V, Koch MA, Beaulieu C, Weiller C, Rother J. Diffusion tensor imaging detects early Wallerian degeneration of the pyramidal tract after ischemic stroke. Neuroimage. 2004; 22:1767–74. [PubMed: 15275932]
9. Sun SW, Liang HF, Cross AH, Song SK. Evolving Wallerian degeneration after transient retinal ischemia in mice characterized by diffusion tensor imaging. Neuroimage. 2008; 40:1–10. [PubMed: 18187343]
10. DeVetten G, Coutts SB, Hill MD, Goyal M, Eesa M, O'Brien B, Demchuk AM, Kirton A. Acute corticospinal tract Wallerian degeneration is associated with stroke outcome. Stroke. 2010; 41:751–6. [PubMed: 20203322]

11. Puig J, Pedraza S, Blasco G, Daunis IEJ, Prats A, Prados F, Boada I, Castellanos M, Sanchez-Gonzalez J, Remollo S, Laguillo G, Quiles AM, Gomez E, Serena J. Wallerian degeneration in the corticospinal tract evaluated by diffusion tensor imaging correlates with motor deficit 30 days after middle cerebral artery ischemic stroke. AJNR Am J Neuroradiol. 2010; 31:1324–30. [PubMed: 20299434]
12. Yu C, Zhu C, Zhang Y, Chen H, Qin W, Wang M, Li K. A longitudinal diffusion tensor imaging study on Wallerian degeneration of corticospinal tract after motor pathway stroke. Neuroimage. 2009; 47:451–8. [PubMed: 19409500]
13. Jang SH, Cho SH, Kim YH, Han BS, Byun WM, Son SM, Kim SH, Lee SJ. Diffusion anisotrophy in the early stages of stroke can predict motor outcome. Restor Neurol Neurosci. 2005; 23:11–7. [PubMed: 15846028]
14. Radlinska B, Ghinani S, Leppert IR, Minuk J, Pike GB, Thiel A. Diffusion tensor imaging, permanent pyramidal tract damage, and outcome in subcortical stroke. Neurology. 2010; 75:1048–54. [PubMed: 20855848]
15. Stinear CM, Barber PA, Petoe M, Anwar S, Byblow WD. The PREP algorithm predicts potential for upper limb recovery after stroke. Brain. 2012; 135:2527–35. [PubMed: 22689909]
16. Basser PJ. Inferring microstructural features and the physiological state of tissues from diffusion-weighted images. NMR Biomed. 1995; 8:333–44. [PubMed: 8739270]
17. Thomalla G, Glauche V, Weiller C, Rother J. Time course of wallerian degeneration after ischaemic stroke revealed by diffusion tensor imaging. J Neurol Neurosurg Psychiatry. 2005; 76:266–8. [PubMed: 15654048]
18. Liang Z, Zeng J, Liu S, Ling X, Xu A, Yu J, Ling L. A prospective study of secondary degeneration following subcortical infarction using diffusion tensor imaging. J Neurol Neurosurg Psychiatry. 2007; 78:581–6. [PubMed: 17237143]
19. Mori S, Crain BJ, Chacko VP, van Zijl PC. Three-dimensional tracking of axonal projections in the brain by magnetic resonance imaging. Ann Neurol. 1999; 45:265–9. [PubMed: 9989633]
20. Heiervang E, Behrens TE, Mackay CE, Robson MD, Johansen-Berg H. Between session reproducibility and between subject variability of diffusion MR and tractography measures. Neuroimage. 2006; 33:867–77. [PubMed: 17000119]
21. Moller M, Frandsen J, Andersen G, Gjedde A, Vestergaard-Poulsen P, Ostergaard L. Dynamic changes of corticospinal tracts after stroke detected by fibertracking. J Neurol Neurosurg Psychiatry. 2007; 78:587–92. [PubMed: 17210628]
22. Schaechter JD, Perdue KL, Wang R. Structural damage to the corticospinal tract correlates with bilateral sensorimotor cortex reorganization in stroke patients. Neuroimage. 2008; 39:1370–82. [PubMed: 18024157]
23. Dawes H, Enzinger C, Johansen-Berg H, Bogdanovic M, Guy C, Collett J, Izadi H, Stagg C, Wade D, Matthews PM. Walking performance and its recovery in chronic stroke in relation to extent of lesion overlap with the descending motor tract. Exp Brain Res. 2008; 186:325–33. [PubMed: 18157670]
24. Schulz R, Park CH, Boudrias MH, Gerloff C, Hummel FC, Ward NS. Assessing the integrity of corticospinal pathways from primary and secondary cortical motor areas after stroke. Stroke. 2012; 43:2248–51. [PubMed: 22764214]
25. Carter AR, Patel KR, Astafiev SV, Snyder AZ, Rengachary J, Strube MJ, Pope A, Shimony JS, Lang CE, Shulman GL, Corbetta M. Upstream dysfunction of somatomotor functional connectivity after corticospinal damage in stroke. Neurorehabil Neural Repair. 2012; 26:7–19. [PubMed: 21803932]
26. Kou N, Park CH, Seghier ML, Leff AP, Ward NS. Can fully automated detection of corticospinal tract damage be used in stroke patients? Neurology. 2013; 80:2242–5. [PubMed: 23658388]
27. Zhu LL, Lindenberg R, Alexander MP, Schlaug G. Lesion load of the corticospinal tract predicts motor impairment in chronic stroke. Stroke. 2010; 41:910–5. [PubMed: 20378864]
28. Stinear CM, Barber PA, Smale PR, Coxon JP, Fleming MK, Byblow WD. Functional potential in chronic stroke patients depends on corticospinal tract integrity. Brain. 2007; 130:170–80. [PubMed: 17148468]

29. Jayaram G, Stagg CJ, Esser P, Kischka U, Stinear J, Johansen-Berg H. Relationships between functional and structural corticospinal tract integrity and walking post stroke. Clin Neurophysiol. 2012; 123:2422–8. [PubMed: 22717679]
30. Tang PF, Ko YH, Luo ZA, Yeh FC, Chen SH, Tseng WY. Tract-specific and region of interest analysis of corticospinal tract integrity in subcortical ischemic stroke: reliability and correlation with motor function of affected lower extremity. AJNR Am J Neuroradiol. 2010; 31:1023–30. [PubMed: 20110374]
31. Petoe MA, Byblow WD, de Vries EJ, Krishnamurthy V, Zhong CS, Barber PA, Stinear CM. A template-based procedure for determining white matter integrity in the internal capsule early after stroke. Neuroimage Clin. 2014; 4:695–700. [PubMed: 24936407]
32. Collin C, Wade D. Assessing motor impairment after stroke: a pilot reliability study. J Neurol Neurosurg Psychiatry. 1990; 53:576–9. [PubMed: 2391521]
33. Cramer SC, Nelles G, Schaechter JD, Kaplan JD, Finklestein SP. Computerized measurement of motor performance after stroke. Stroke. 1997; 28:2162–8. [PubMed: 9368558]
34. Mathiowetz V, Weber K, Kashman N, Volland G. Adult norms for the nine hole peg test of manual dexterity. Occup Ther J Res. 1985; 5:24–37.
35. Fugl-Meyer AR, Jaasko L, Leyman I, Olsson S, Steglind S. The post-stroke hemiplegic patient: a method for the evaluation of physical performance. Scand J Rehabil Med. 1975; 7:13–31. [PubMed: 1135616]
36. Gladstone DJ, Danells CJ, Black SE. The fugl-meyer assessment of motor recovery after stroke: a critical review of its measurement properties. Neurorehabil Neural Repair. 2002; 16:232–40. [PubMed: 12234086]
37. FDT. http://www.fmrib.ox.ac.uk/fsl/fdt
38. DTK. http://trackvis.org/dtk
39. Trackvis. http://trackvis.org
40. Freesurfer. http://surfer.nmr.mgh.harvard.edu
41. Greve DN, Fischl B. Accurate and robust brain image alignment using boundary-based registration. Neuroimage. 2009; 48:63–72. [PubMed: 19573611]
42. Mori S, Oishi K, Faria AV. White matter atlases based on diffusion tensor imaging. Curr Opin Neurol. 2009; 22:362–9. [PubMed: 19571751]
43. FSL. http://www.fmrib.ox.ac.uk/fsl
44. Wakana S, Caprihan A, Panzenboeck MM, Fallon JH, Perry M, Gollub RL, Hua K, Zhang J, Jiang H, Dubey P, Blitz A, van Zijl P, Mori S. Reproducibility of quantitative tractography methods applied to cerebral white matter. Neuroimage. 2007; 36:630–44. [PubMed: 17481925]
45. Meng XL, Rosenthal R, Rubin DB. Comparing correlated correlation coefficients. Psychological Bulletin. 1992; 111:172–5.
46. Benjamini Y, Hochberg Y. Controlling the false discovery rate: a practical and powerful approach to multiple testing. J R Statist Soc B. 1995; 57:289–300.
47. FDR. http://www.sdmproject.com/utilities/?show=FDR
48. Schwamm LH, Koroshetz WJ, Sorensen AG, Wang B, Copen WA, Budzik R, Rordorf G, Buonanno FS, Schaefer PW, Gonzalez RG. Time course of lesion development in patients with acute stroke: serial diffusion- and hemodynamic-weighted magnetic resonance imaging. Stroke. 1998; 29:2268–76. [PubMed: 9804633]
49. Beaulieu C, de Crespigny A, Tong DC, Moseley ME, Albers GW, Marks MP. Longitudinal magnetic resonance imaging study of perfusion and diffusion in stroke: evolution of lesion volume and correlation with clinical outcome. Ann Neurol. 1999; 46:568–78. [PubMed: 10514093]
50. Werring DJ, Toosy AT, Clark CA, Parker GJ, Barker GJ, Miller DH, Thompson AJ. Diffusion tensor imaging can detect and quantify corticospinal tract degeneration after stroke. J Neurol Neurosurg Psychiatry. 2000; 69:269–72. [PubMed: 10896709]
51. Hua K, Zhang J, Wakana S, Jiang H, Li X, Reich DS, Calabresi PA, Pekar JJ, van Zijl PC, Mori S. Tract probability maps in stereotaxic spaces: analyses of white matter anatomy and tract-specific quantification. Neuroimage. 2008; 39:336–47. [PubMed: 17931890]

52. Thomas B, Eyssen M, Peeters R, Molenaers G, Van Hecke P, De Cock P, Sunaert S. Quantitative diffusion tensor imaging in cerebral palsy due to periventricular white matter injury. Brain. 2005; 128:2562–77. [PubMed: 16049045]

53. Vargas P, Gaudron M, Valabregue R, Bertasi E, Humbert F, Lehericy S, Samson Y, Rosso C. Assessment of corticospinal tract (CST) damage in acute stroke patients: comparison of tract-specific analysis versus segmentation of a CST template. J Magn Reson Imaging. 2013; 37:836–45. [PubMed: 23086724]

54. Seghier ML, Ramlackhansingh A, Crinion J, Leff AP, Price CJ. Lesion identification using unified segmentation-normalisation models and fuzzy clustering. Neuroimage. 2008; 41:1253–66. [PubMed: 18482850]

55. Lin GC, Wang WJ, Kang CC, Wang CM. Multispectral MR images segmentation based on fuzzy knowledge and modified seeded region growing. Magn Reson Imaging. 2012; 30:230–46. [PubMed: 22133286]

56. Jones DK. Studying connections in the living human brain with diffusion MRI. Cortex. 2008; 44:936–52. [PubMed: 18635164]

57. Farquharson S, Tournier JD, Calamante F, Fabinyi G, Schneider-Kolsky M, Jackson GD, Connelly A. White matter fiber tractography: why we need to move beyond DTI. J Neurosurg. 2013; 118:1367–77. [PubMed: 23540269]

58. Kristo G, Leemans A, Raemaekers M, Rutten GJ, de Gelder B, Ramsey NF. Reliability of two clinically relevant fiber pathways reconstructed with constrained spherical deconvolution. Magn Reson Med. 2013; 70:1544–56. [PubMed: 23359402]

Highlights

- New DTI-based density-weighted CST template approach for measuring CST injury.
- Predict motor outcome of acute stroke patients with severe impairment by CST injury.
- Compared prediction by injury measured using new versus common DTI-based approaches.
- Stronger prediction by new DTI-based density-weighted CST template approach.

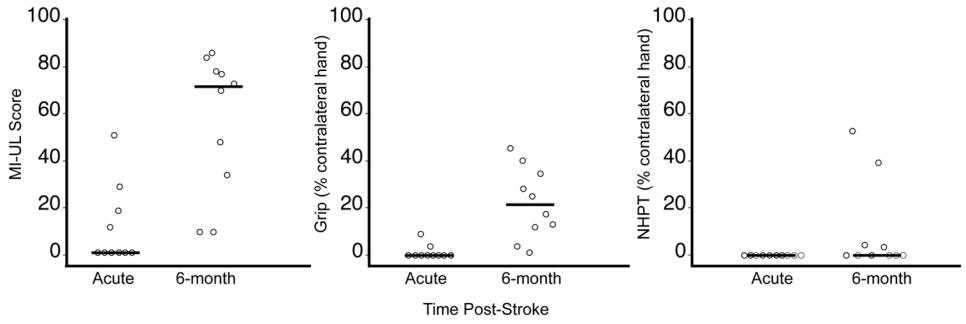

Figure 1.

Motor functions of the paretic upper limb of stroke patients at the acute and 6-month time points. Symbols have been shifted along x-axis to allow easier visualization. The line at each time point represents the median. Patients made significant gains in MI-UL and grip (each $P < 0.01$, Wilcoxon Signed Rank), but not NHPT ($P = 0.125$).

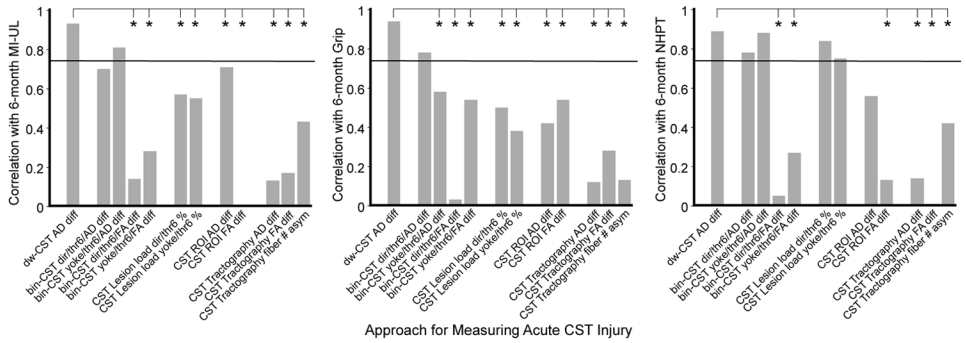

Figure 2.

Correlations between 6-month motor functions and acute CST injury measurements made by the density-weighted CST template approach and several alternative approaches with their variants. Values are Spearman's correlation coefficients, in absolute r_s. The horizontal lines indicate the threshold correlation for significance ($r_s = 0.75$, FDR-corrected $P < 0.05$). Meng's test was used to compare correlation strength of AD difference measurements made by the density-weighted CST template approach versus each alternative measurement. * FDR-corrected $P < 0.05$

Table 1

Patient Characteristics

				Stroke Characteristics			
Patient	**Age**	**Gender**	**Premorbid Handedness**	**Hemisphere**	**Location**	**Etiology (CCS)**	**Medical Intervention**
1	19	F	R	R	> 1/3 MCA territory	Unknown (cryptogenic)	IV rTPA and IA therapy
2	52	F	R	R	> 1/3 MCA territory	Other (CAD)	
3	55	F	R	L	> 1/3 MCA territory	Other (CAD)	
4	64	M	R	R	> 1/3 MCA territory	Other (CAD)	
5	50	F	R	R	> 1/3 MCA territory	Cardio-aortic embolism	IV rTPA and IA therapy
6	49	M	R	L	> 1/3 MCA territory	Large artery atherosclerosis	
7	62	M	R	R	Precentral and postcentral gyri, temporal lobe	Large artery atherosclerosis	IV rTPA
8	59	M	R	R	CR, IC, BG, insula	Large artery atherosclerosis	IV rTPA and carotid endarterectomy
9	49	M	R	R	CR, IC	Small artery occlusion	
10	67	F	R	R	CR, IC, BG	Large artery atherosclerosis	IV rTPA

M = male; F = female; R = right; L = left; CCS = Causative Classification System; MCA = middle cerebral artery; IV rTPA = intravenous recombinant tissue plasminogen activator; IA = intra-arterial; CAD = carotid artery dissection; CR = corona radiata; IC = internal capsule; BG = basal ganglia

Table 2

Within-approach correlations of acute CST injury measurements

	Bin-CST direct/thr6/AD diff	Bin-CST direct/thr8/AD diff	Bin-CST direct/thr6/AD asym	Bin-CST direct/thr8/AD asym	Bin-CST yoke/thr6/AD diff	Bin-CST yoke/thr8/AD diff	Bin-CST yoke/thr6/AD asym	Bin-CST yoke/thr8/AD asym	Bin-CST direct/thr6/FA diff	Bin-CST direct/thr8/FA diff	Bin-CST direct/thr6/FA asym	Bin-CST direct/thr8/FA asym	Bin-CST yoke/thr6/FA diff	Bin-CST yoke/thr8/FA diff	Bin-CST yoke/thr6/FA asym	Bin-CST yoke/thr8/FA asym	CST LL direct/ thr6 %	CST LL yoke/ thr8 %	CST LL yoke/ thr6 %	CST LL yoke/ thr8 %	CST ROI AD diff	CST ROI AD asym	CST ROI FA diff	CST ROI FA asym	CST Tractography AD diff	CST Tractography AD asym	CST Tractography FA diff	CST Tractography FA asym	CST Tractography fiber# asym
Bin-CST direct/thr6/AD diff		**0.96**	**0.99**	**0.96**	**0.77**	0.72	**0.82**	**0.73**	0.13	0.12	0.21	0.29	0.54	0.45	0.55	0.52													
Bin-CST direct/thr8/AD diff			**0.94**	**1.00**	**0.79**	**0.75**	**0.83**	**0.76**	0.03	0.05	0.01	0.07	0.45	0.37	0.44	0.39													
Bin-CST direct/thr6/AD asym				**0.94**	**0.75**	0.71	**0.81**	0.71	0.16	0.14	0.22	0.31	0.58	0.49	0.60	0.56													
Bin-CST direct/thr8/AD asym					**0.79**	**0.75**	**0.83**	**0.76**	0.03	0.05	0.01	0.07	0.45	0.37	0.44	0.39													
Bin-CST yoke/thr6/AD diff						**0.97**	**0.99**	**0.96**	0.09	0.02	0.07	0.02	0.21	0.14	0.25	0.21													
Bin-CST yoke/thr8/AD diff							**0.94**	**1.00**	0.19	0.11	0.13	0.05	0.30	0.22	0.32	0.26													
Bin-CST yoke/thr6/AD asym								**0.94**	0.04	0.01	0.09	0.05	0.22	0.15	0.26	0.25													
Bin-CST yoke/thr8/AD asym									0.18	0.12	0.12	0.07	0.30	0.21	0.31	0.26													
Bin-CST direct/thr6/FA diff										**0.96**	**0.81**	**0.84**	0.67	0.68	0.72	**0.73**													
Bin-CST direct/thr8/FA diff											**0.83**	**0.92**	0.61	0.62	0.65	0.72													
Bin-CST direct/thr6/FA asym												**0.90**	0.61	0.63	0.67	0.71													
Bin-CST direct/thr8/FA asym													0.66	0.67	0.71	**0.82**													
Bin-CST yoke/thr6/FA diff														**0.99**	**0.99**	**0.94**													
Bin-CST yoke/thr8/FA diff															**0.98**	**0.95**													
Bin-CST yoke/thr6/FA asym																**0.95**													
Bin-CST yoke/thr8/FA asym																													
CST LL direct/thr6 %																		**0.96**	**0.92**	**0.88**									
CST LLdirect/thr8 %																			**0.89**	**0.85**									
CST LLyoke/thr6 %																				**0.94**									
CST LL yoke/thr8 %																													
CST ROI AD diff																						**1.00**	0.15	0.15					
CST ROI AD asym																							0.15	0.15					
CST ROI FA diff																								**1.00**					
CST ROI FA asym																													
CST Tractography AD diff																										**0.98**	0.47	0.47	0.38
CST Tractography AD asym																											0.43	0.43	0.34
CST Tractography FA diff																												**1.00**	0.27
CST Tractography FA asym																													0.27
CST Tractography fiber# asym																													

Values are Spearman's correlation coefficients, in absolute value. Bolded values are significant at FDR-corrected P < 0.05. bin-CST, binary CST template; direct, direct normalization method; yoke, yoke normalization method; thr6, 6 of 12 subject overlap; thr8, 8 of 12 subject overlap; diff, difference metric; asym, asymmetry metric; LL, lesion load

Table 3

Between-approach correlations

	Correlation with dw-CST AD diff		
	r_s	uncor P	FDR-cor P
bin-CST direct/thr6/AD diff	0.80	0.01	0.06
bin-CST yoke/thr6/AD diff	0.76	0.01	0.06
bin-CST direct/thr6/FA diff	0.16	0.66	0.73
bin-CST yoke/thr6/FA diff	0.39	0.27	0.49
CST LL direct/thr6 %	0.62	0.05	0.20
CST LL yoke/thr6 %	0.54	0.11	0.24
CST ROI AD diff	0.58	0.08	0.21
CST ROI FA diff	0.27	0.46	0.63
CST Tractography AD diff	0.09	0.82	0.82
CST Tractography FA diff	0.21	0.57	0.69
CST Tractography fiber # asym	0.36	0.31	0.49